iScience

CellPress
OPEN ACCESS

Article

Conversion of glioma cells into neuron-like cells by small molecules

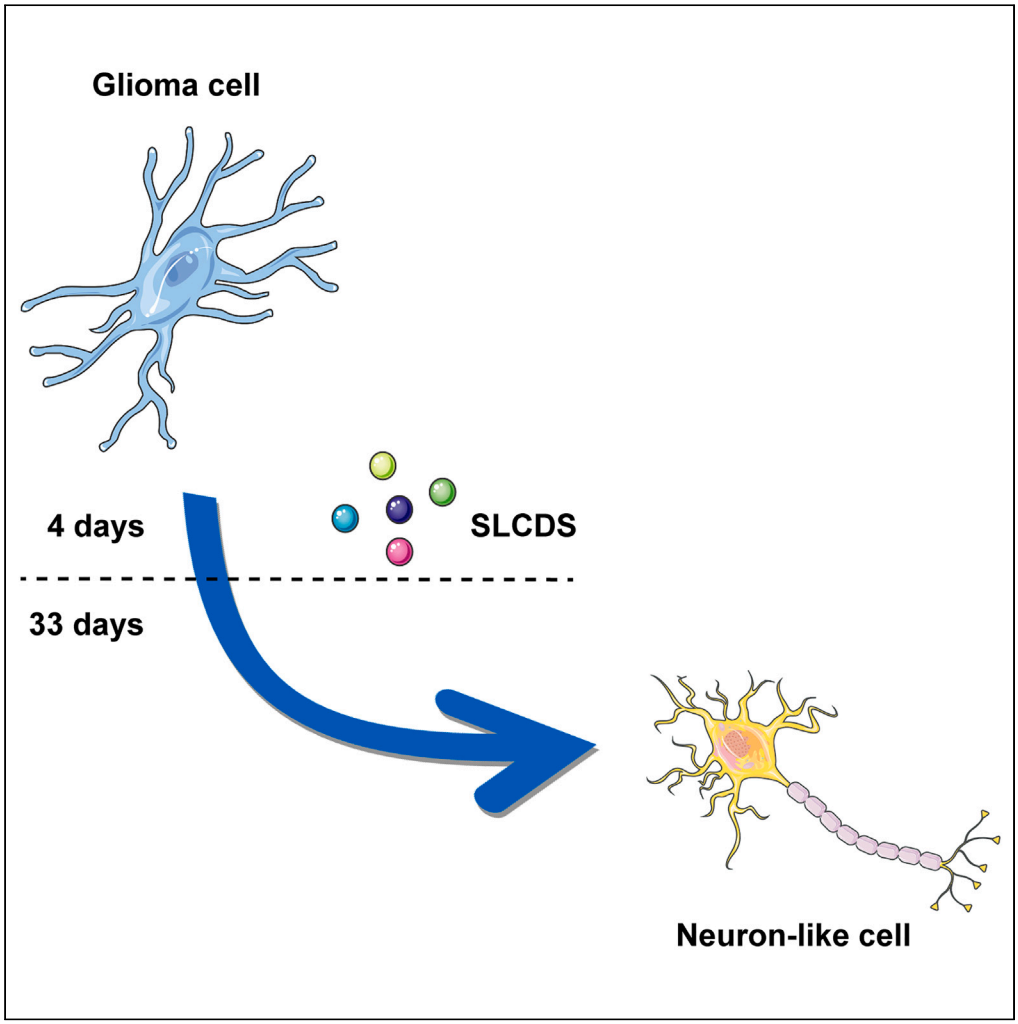

Yongjun Yi, Wenqiang Che, Ping Xu, ..., Qingsong Wang, Jun Lyu, Xiangyu Wang

wqshty@163.com (Q.W.)
lyujun2020@jnu.edu.cn (J.L.)
wang_xy123@126.com (X.W.)

Highlights

SLCDS has been shown to convert human glioma cells into mature neuron-like cells

SLCDS inhibits the expressions of EGFR, PDGFR, Ki67, and vimentin in gliomas

NTFs and genes linked to neurogenesis and tumor suppression were upregulated

Overexpressing nTFs can induce the conversion of glioma cells into neuronal cells

Yi et al., iScience *27*, 111091
November 15, 2024
https://doi.org/10.1016/j.isci.2024.111091

iScience

CellPress
OPEN ACCESS

Article

Conversion of glioma cells into neuron-like cells by small molecules

Yongjun Yi,[1,3,7] Wenqiang Che,[2,3,7] Ping Xu,[4,7] Chuxiao Mao,[5] Zhizhong Li,[4] Qingsong Wang,[5,*] Jun Lyu,[6,*] and Xiangyu Wang[3,8,*]

SUMMARY

Currently, researchers are exploring the conversion of astrocytes into functional mature neurons and gradually exploring the conversion of glioma into neurons. We report that SLCDS (SB431542, LDN193189, CHIR99021, DAPT, and SKL2001) has been shown to convert human glioma cells into mature neuron-like cells. The converted cells exhibited upregulation of DCX, TuJ1, MAP2, NeuN, and GAD67, while the expressions of EGFR, PDGFR, Ki67, and vimentin were inhibited. The nTFs, such as NeuroD1 and Sox2, were upregulated, along with TF genes associated with neurogenesis and tumor suppression. We have finally confirmed that overexpressing nTFs can induce the conversion of glioma cells into neuronal cells. This study demonstrates that SLCDS can activate the expression of nTFs in human glioma cells and induce the conversion of human glioma cells into neuron-like cells. Additionally, SLCDS inhibits the expressions of EGFR, PDGFR, Ki67, and Vimentin in gliomas. Our findings offer a potential approach for treating glioma.

INTRODUCTION

Neuronal conversion technology holds great promise to treat neurological disorders, especially glioma. Gliomas are the most frequent primary tumors of the central nervous system, but the prognosis of most patients is not ideal.[1,2] In 2012, Jiao Jianwei infected human primary glioma cells, U251 and U87 glioma cell lines, with lentivirus carrying three transcription factors coding for ASCL1, Brn2, and Neurog2, and the infected glioma cells gradually showed neuron-like changes and expressed markers of partially early or immature neurons.[3] Since then, more researchers have started trying to convert gliomas, especially low-grade gliomas such as U251, into functional mature neurons by transfecting multiple or even a single neuronal transcription factor encoding.[4–7] However, there are limitations to the therapeutic feasibility of high-grade gliomas and conversion efficiency, and the overall inhibitory effect on gliomas is not obvious. In 2013, Deng Hongkui's team reported a major breakthrough, using small molecules for the first time to reprogram somatic cells into multipotent stem cells.[8] Researchers realized that small molecules possess reprogramming capabilities similar to transcription factors, but with simpler applications, lower cost, and greater safety. Small molecules were utilized in the research of various neurological diseases, such as Alzheimer's disease, glioma, etc., to convert astrocytes, fibroblasts, or glioma cells into neuron-like cells.[9,10] The Yoon Ha team in Korea reported in 2017 that two small molecules (Forskolin and CHIR99021) successfully converted rat C6 glioma cells to early neurons by regulating cAMP and GSK3 signaling pathways,[11] marking the first instance of small molecules being used in glioma neuronal conversion. Subsequently, the Stephanie M. Willerth team also reported five small molecules (Forskolin, ISX9, CHIR99021, I-BET 151, and DAPT) that induced the conversion of human glioblastoma U87 into early neurons, upregulating the Ngn2, Ascl1, Brn2, and MAP2 genes.[12] Although the converted cells could only develop to an early stage and the mechanisms behind this converting phenomenon are unexplored, these findings also indicate the potential of small molecules in converting glioma cells into neurons.

A combination of CORE (SB431542, LDN193189, CHIR99021, and DAPT) was found to efficiently convert human astrocytes into neurons.[13] In this study, we reported a small molecule combination of SB431542, LDN193189, CHIR99021, DAPT, combined with SKL2001 (SLCDS) that specifically modulated cell signaling pathways such as Notch, TGF- β/Smads, and Wnts/β-Catenin,[14–18] proved to convert human glioma cells

[1]Department of Neurosurgery, Zhujiang Hospital, Southern Medical University, The National Key Clinical Specialty, The Engineering Technology Research Center of Education Ministry of China, Guangdong Provincial Key Laboratory on Brain Function Repair and Regeneration, The Neurosurgery Institute of Guangdong Province, Guangzhou 510632, P.R. China
[2]Department of Neurosurgery, Guangdong Cardiovascular Institute, Guangdong Provincial People's Hospital (Guangdong Academy of Medical Sciences), Southern Medical University, Guangzhou 510080, P.R. China
[3]Department of Neurosurgery, The First Affiliated Hospital of Jinan University, Guangzhou 510630, P.R. China
[4]Department of Orthopedics, The First Affiliated Hospital of Jinan University, Guangzhou 510630, P.R. China
[5]Guangdong-Hongkong-Macau CNS Regeneration Institute of Jinan University, Key Laboratory of CNS Regeneration (Jinan University)-Ministry of Education, Guangdong Key Laboratory of Non-human Primate Research, Guangzhou 510630, P.R. China
[6]Department of Clinical Research, The First Affiliated Hospital of Jinan University, Guangzhou 510632, P.R. China
[7]These authors contributed equally
[8]Lead contact
*Correspondence: wqshty@163.com (Q.W.), lyujun2020@jnu.edu.cn (J.L.), wang_xy123@126.com (X.W.)
https://doi.org/10.1016/j.isci.2024.111091

into mature neurons. Multiple neural transcription factors were found to be upregulated in the converted cells during the conversion process, and researchers also observed a marked suppression of proteins associated with neoplastic properties. Additionally, SLCDS induced significant changes in gene expression in glioma, upregulating biological functions related to neurogenesis and suppressing those related to glioma. Among the differential genes, a series of transcription factors closely related to neurogenesis and tumor suppression were upregulated, and these transcription factors were involved in regulating most differential genes. We thus experimented with forced upregulation of some classical neural transcription factors in various glioma cells and found that gliomas all exhibited different degrees of conversion to neurons. We demonstrated that the upregulation of neural transcription factors by SLCDS may be linked to these conversion effects. Taken together, our study demonstrates the feasibility of small molecules induced neuronal conversion to treat gliomas.

RESULTS

Conversion of human glioma cells into neuron-like cells by small molecules

Several groups have used small molecules to convert astrocytes into neurons. In our previous study, we demonstrated that four core small molecules (CHIR99021, DAPT, LDN193189, and SB431542) can efficiently convert human astrocytes into functional neurons.[13] Therefore, we named these four small molecules CORE, and applied CORE to induce glioma cells for neuronal conversion. Previous results showed that glioma cells converted into early neuron-like cells, but none of them eventually converted into mature neurons.

We then tested several combinations based on CORE, and found that CORE + SKL2001 induced a significant increase in the number of DCX-positive cells in U251 glioma at an early stage (14 days past induction, DPI), and the number of DCX (+) cells increased with increasing concentrations of SKL2001. The DCX expression increased significantly at 40 μM and 80 μM, and paradoxically showed a decreasing trend when the concentration increased to 160 μM (Figure 1A). At 14 DPI, U251 cells exhibited morphological changes mainly characterized by retraction and rounding of the cell soma, initiation of monopolar axon formation, and attachment of morphologically altered cells to the unaltered cell layer. An increased number of cells with altered morphology was observed at 21 DPI, and the prominence of the "neuron-like" morphology, characterized by rounded cell bodies and elongated axons, was more evident. The greater number of converted cells was observed at 28 DPI, showing more typical "neuron-like" cells that were monopolar or bipolar, while control cells still retained their characteristic glioma cell morphology (Figure 1B). We examined neuronal markers at 21 DPI. After CORE induction without SKL2001, early neuronal marker DCX (+) cells was observed, but there was no significant expression of the immature neuronal marker TuJ1 and the specific neuronal marker MAP2. In contrast, DCX expression in cells induced by SLCDS was significantly reduced compared to 14 DPI, with TuJ1 and MAP2 beginning to be expressed. In addition, some cells appeared to express DCX, TuJ1, and MAP2 (Figure 1C). Furthermore, the number of glioma cells induced by SLCDS was demonstrably lower than that induced by CORE. At 28 DPI, DCX expression was further reduced in cells induced by SLCDS and CORE. No obvious DCX expression was observed in cells induced by SLCDS, but it was significantly increased in the number of MAP2 (+) cells compared to before. The trend of upregulation of MAP2 expression and downregulation of DCX expression under SLCDS induction at 2× concentration appeared to be more pronounced. The neuron-like morphology became increasingly complex with the conversion of an increasing number of multipolar cells (Figures 1D, 1E, and 1F). CORE-induced cells also began to show MAP2 expression at 28 DPI, but the number of MAP2 (+) cells was significantly lower than that induced by SLCDS. Changes in these neuronal markers reflect a stepwise transition of converted cells from a naive state to mature neuron-like cells.

At 37 DPI, expression of the mature neuronal marker NeuN was significantly higher in SLCDS-induced cells compared to CORE-induced cells and controls. The NeuN (+)/DAPI (+) ratio was approximately 10% (9.7% ± 1.1%; $p < 0.01$). In addition, there was a strong expression of MAP2, and interconnected MAP2 (+) cells were observed to form a meshwork with elongated cellular protrusions in large areas (Figures 2A, 2B, and 2C). Although there was significant MAP2 expression in CORE-induced cells, the number of MAP2 (+) cells was relatively small. These MAP2 (+) cells were also significantly less connected by cell protrusions, and no positive expression of NeuN was observed, indicating that the converted cells were still immature. We further examined neuronal subtype markers and found that at 40 DPI, SLCDS-induced cells showed expression of the GABAergic neuron marker GAD67 and no expression of the glutamatergic neuron marker VGLUT2 (Figure 2D).

SLCDS inhibited tumor-associated proteins in glioma cells

We observed a general phenomenon in which SLCDS-induced U251 cells tended to have a significantly lower cell density and slower proliferation compared to the control and CORE-induced cells. We hypothesized that SLCDS might have an inhibitory effect on glioma cells, so we tested some antigenic markers commonly expressed by gliomas. At 7 DPI, cells treated with CORE for 4 days or 7 days showed reduced EGFR expression intensity compared to controls. In particular, cells induced with SLCDS showed reduced EGFR expression compared to both controls and CORE. Especially at a concentration of 2 ×, only a very weak expression of EGFR was observed in SLCDS-induced cells. EGFR expression decreased in cells after 7 days of incubation compared to 4 days of incubation. Meanwhile, there was no expression of DCX after 4 days of incubation. However, DCX (+) cells appeared after 7 days of incubation with 2 × SLCDS and showed early neuron-like cellular changes (Figures 3A and 3B). Furthermore, the cell count was lower under SLCDS induction compared to the CORE and control groups (4 days of incubation 265 ± 14; 7 days of incubation 601 ± 49), with the cell density in the 2 × SLCDS group being the lowest (4 days of incubation 257 ± 12; 7 days of incubation 95 ± 16; Figures 3C and 3D). We also examined the expression of PDGFR, another common antigenic marker for glioma, the platelet-derived growth factor receptor. At 7 DPI, PDGFR expression was present in almost all cells in the control group after 4 days of incubation, with very pronounced PDGFR expression in some cells. In contrast, very weak PDGFR expression was observed in SLCDS-induced cells (Figure 3E). We also performed immunofluorescence staining for vimentin, a protein closely associated with tumor metastasis. At 31 DPI, a higher number of tumor cells in the control group showed strong vimentin expression, whereas vimentin expression

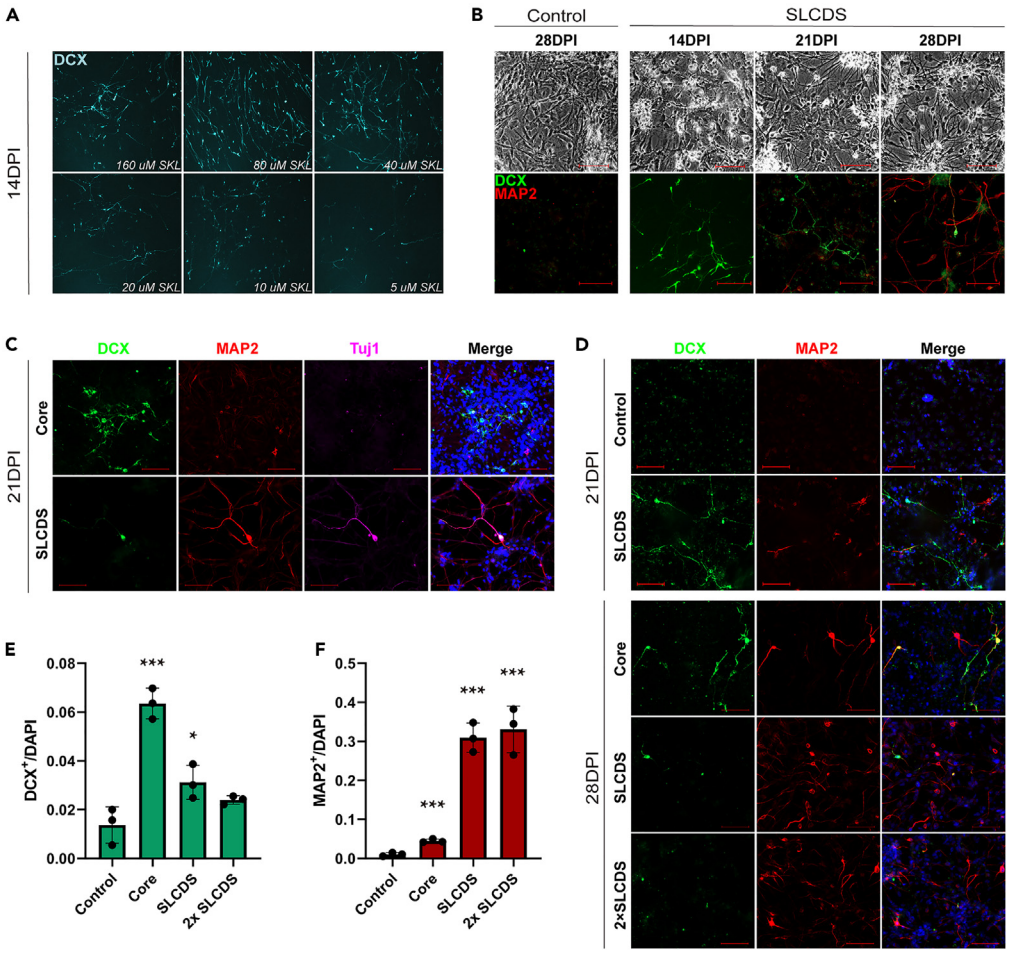

Figure 1. Neuronal-like conversion of glioma cells by treatment with small molecules

(A) The expression of DCX was observed under a concentration gradient of SKL2001 with CORE in U251 cells, 14 days post induction (DPI).

(B) The morphological changes in the bright field and the immunofluorescence of DCX and MAP2 at 14 DPI, 21DPI, and 28 DPI with SLCDS in U251 cells. The scale bar: 100 μm.

(C) The expression of multiple neuronal markers in the CORE and SLCDS groups at 21 DPI. Scale bar: 100 μm.

(D) SLCDS showed more mature neuron-like cells than CORE when inducing the conversion of U251 cells. Scale bar: 100 μm. (E and F) Quantitative analysis of DCX (+)/DAPI and MAP2 (+)/DAPI in each group at 28 DPI, data were represented as mean ± SEM. $n = 3$; *$p < 0.05$; ***$p < 0.001$; One-way ANOVA followed by Dunnett's multiple comparison test.

in the CORE group was reduced compared to the control group. Vimentin expression was further reduced in the SLCDS group, and the cell density was significantly lower. In addition, MAP2 (+) was not co-labeled with vimentin (+) (Figure 3F). Ki67 expression, which is used to assess cell proliferation activity, was also examined. The results showed that at 28 DPI, Ki67 expression was highly active in control cells, with a Ki67 (+)/DAPI (+) ratio close to 60% (56.5% ± 12.0%). However, it was significantly reduced in cells induced by CORE and SLCDS. The most notable decrease was observed following 4 days of incubation with 2 × SLCDS, with the Ki67 (+)/DAPI (+) ratio decreasing to below 20% (9.0% ± 1.8%). Similar reductions of almost 20% were also observed (see Figures 4B and 4C for details). We observed that the expression of Ki67 was lower in the SLCDS group than in the control group at 14 DPI and 21 DPI (Figure 4E).

Upregulation of neural transcription factors by SLCDS in neuronal conversion

We also observed an increase in the expression of certain transcription factors closely associated with neurodevelopment at various times during small-molecule-induced conversion. At 21 DPI, U251 cells had undergone significant changes in cell morphology, with the converted cells interconnected in a meshwork (Figure 4A). A large number of TuJ1 (+) cells were observed in the SLCDS-induced glioma cells. In addition, many TuJ1 (+) converted cells also showed significant expression of the bHLH neural transcription factor NeuroD1. Nearly all NeuroD1 (+) cells co-labeled with TuJ1 (+) cells, and showed a converted morphology. At 28 DPI (Figures 4B and 4D), no significant expression of MAP2 and Sox2 was observed in the control group. However, cells incubated with CORE for 4 days showed an increase in MAP2 expression, with

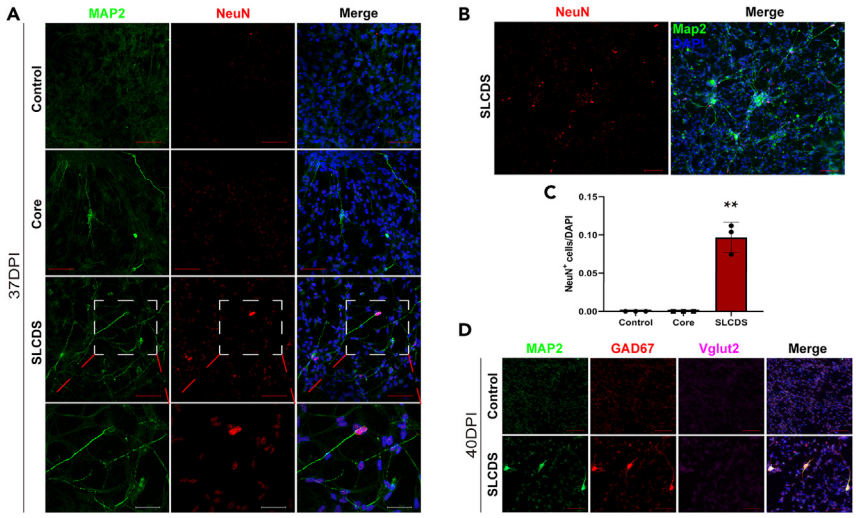

Figure 2. The mature neuron-like cells with SLCDS in U251 cells

(A) The expression of MAP2 and NeuN and the morphology of the converted cells in SLCDS-induced U251 cells at 37 DPI. Red scale bar: 100 μm, white scale bar: 50 μm.

(B) Both NeuN (+) and MAP2 (+) neuron-like cells appeared in SLCDS-induced U251 cells at 37 DPI. Scale bar: 100 μm.

(C) Quantitative analysis of NeuN (+) cells/DAPI in each group at 37 DPI, data were represented as mean ± SEM. $n = 3$; $^{**}p < 0.01$; One-way ANOVA followed by Dunnett's multiple comparison test.

(D) The neuron-like cells in U251 cells at 40 DPI showed GABAergic neuron marker GAD67 (+) expression with SLCDS, with a scale bar: 100 μm.

sporadic cells showing high MAP2 expression and neuron-like cell morphology, but no significant expression of Sox2. Compared to the CORE group and control groups, cells incubated with SLCDS for 4 days showed an increase in MAP2 expression, with a higher number of MAP2 (+) cells, and Sox2 expression started to increase, with occasional appearance of Sox2 (+) cells (25.4% ± 4.9%). Furthermore, compared to the previous three groups, the number of MAP2 (+) cells in cells incubated with 2x SLCDS for 4 days continued to increase, with more cells displaying a clear pattern of high MAP2 expression and neuron-like cell morphology. Overall, Sox2 expression was higher, with more Sox2 (+) cells appearing in this group (26.0% ± 3.9%). After treatment with 2x SLCDS for 7 days, there was an increase in MAP2 expression in more cells, but fewer cells showed high levels of MAP2 expression compared to the other experimental groups. In addition, Sox2 expression was significantly upregulated in comparison to all other groups, resulting in an increase in the number of Sox2 (+) cells (50.0% ± 1.7%). Notably, high MAP2 expression rarely co-labeled with Sox2 and Ki67 positive on the same cells, but some cells with lower MAP2 expression co-labeled with Sox2 positive, and Ki67 appeared on some cells. The high and low expression of MAP2 may distinguish two types of cells at different stages of conversion, and it is possible that some of the MAP2 low (+)/Sox2 (+) cells were converted into neural progenitor-like cells. The neural transcription factors NeuroD1 and Sox2 were highly expressed in U251 cells following SLCDS induction, and these transcription factors were expressed in almost all converted cells.

SLCDS upregulated the expression of neural-associated transcription factors, promoted neurogenesis, and repressed genes associated with tumor

Finally, we performed high-throughput sequencing of transcriptome expression at 14DPI using SLCDS in U251 cells. The cells are currently in the intermediate stages of transition from glioma cells to neurons. The results showed 414 differentially expressed protein-coding genes, with 343 genes showing upregulation and 71 genes showing downregulation (Figure 5A). The statistically significant genes were determined by $p < 0.05$ and log2 FC > 1.0. The expression levels of these differentially expressed genes were significantly different between the SLCDS and control groups (Figure 5C, genes with a q-value <0.05 and |log2 FC| > 1.0 were counted to plot the Heatmap). Channel enrichment analysis of the Reactome database revealed that the 71 downregulated genes were mainly enriched in pathways such as G-protein-coupled receptor and its downstream pathways, interleukin-13 signaling pathway, and receptor tyrosine kinases. These signaling pathways are closely associated with glioma development and progression and are primarily involved in tumor signaling, proliferation, invasion and migration, and angiogenesis. On the other hand, the upregulated genes were mainly associated with neuronal conversion or neurogenesis, including nervous system development, axonal growth guidance, membrane potential and action potential, sensory function, extracellular matrix remodeling, cell cycle regulation, cell cycle control, chromosome unwinding, etc.(Figures 5B and 5C). By comparing the distribution of transcription factors across the entire gene and the differentially expressed genes (up- and downregulated), transcription factors with significant differences in proportion can be identified (see Figure 6A). Among all the differentially expressed genes, we observed a significant upregulation of a series of transcription factor genes. The downstream targets of these transcription factors were found to be associated with most of the differentially expressed genes mentioned above (Figures 6B and 6C). Among these transcription factors, the zf-C2H2 and PAX family

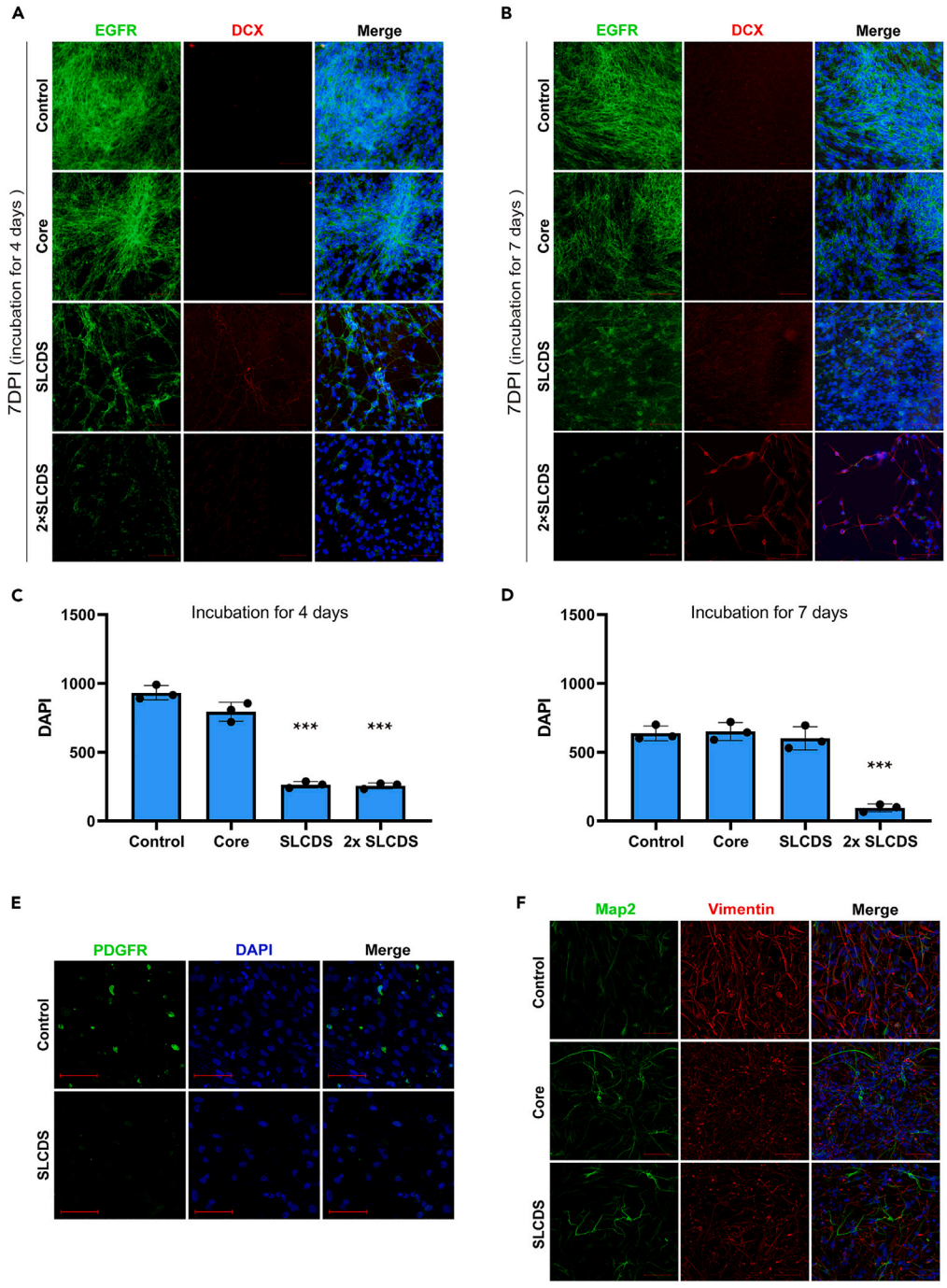

Figure 3. The expression of tumor associated proteins was inhibited in U251 cells with SLCDS

(A) The expression of EGFR, a tumor marker, was observed in different groups after 4 days of incubation in U251 cells at 7 DPI. The scale bar is 100 μm.

(B) The expression of EGFR was also inhibited when SLCDS was incubated for 7 days in U251 cells, while the expression of DCX was upregulated. Scale bar is 100 μm.

(C) Quantitative analysis of DAPI in each group after 4 days of incubation at 7 DPI, data were represented as mean ± SEM. $n = 3$; ***$p < 0.001$; One-way ANOVA followed by Dunnett's multiple comparison test.

(D) Quantitative analysis of DAPI in each group after 7 days of incubation at 7 DPI, data were represented as mean ± SEM. $n = 3$; ***$p < 0.001$; One-way ANOVA followed by Dunnett's multiple comparison test.

(E) SLCDS inhibited the expression of PDGFR in U251 cells at 7 DPI. The scale bar is 100 μm.

(F) SLCDS inhibited vimentin expression in U251 cells at 31 DPI. The scale bar is 100 μm.

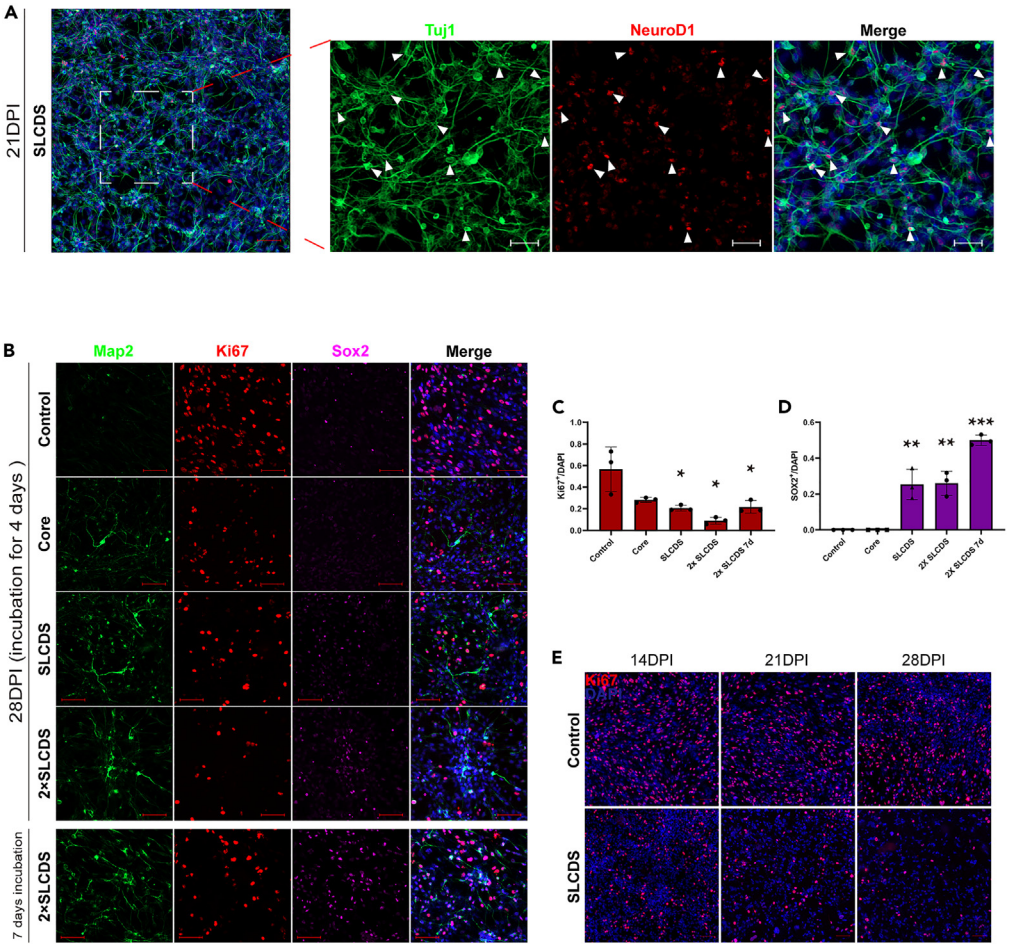

Figure 4. The upregulation of neural transcription factor and the downregulation of cell proliferation activity in SLCDS-induced neuronal conversion

(A) TuJ1 (+) converted cells also exhibited the expression of NeuroD1 in the SLCDS-induced cells at 21 DPI. The scale bar is100 μm.

(B) SLCDS upregulated Sox2 and inhibited Ki67 expression in U251 cells at 28 DPI. The scale bar is 100 μm.

(C) Quantitative analysis of Ki67(+) cells/DAPI in each group at 28 DPI, data were represented as mean ± SEM. $n = 3$; *$p < 0.05$; One-way ANOVA followed by Dunnett's multiple comparison test.

(D) Quantitative analysis of Sox2(+) cells/DAPI in each group at 28 DPI, data were represented as mean ± SEM. $n = 3$; **$p < 0.01$; ***$p < 0.001$; One-way ANOVA followed by Dunnett's multiple comparison test.

(E) The expression of Ki67 was lower in the SLCDS group than in the control group at 14 DPI, 21 DPI, and 28 DPI, scale bar: 100 μm.

transcription factors that affected the most targeted genes were KLF15, EGR2, and PAX5, respectively, all of which are closely related to neurodevelopment.[19–27] Meanwhile, the ETS family transcription factors included ETV4, ETV5, and EHF, ETV4 and ETV5 were implicated in neurodevelopment,[28–32] while EHF, which was a tumor suppressor in the organism, was an alternative tumor suppressor gene to p53.[33–37]

Overexpression of neural transcription factors induced glioma-to-neuron conversion

We synthesized retrovirus and inserted GFP, NeuroD1-GFP, and ASCL1-GFP coding into the viral vector. We selected CAG as the promoter to synthesize Retrovirus CAG-GFP (RV-CAG-GFP), Retrovirus CAG:ASCL1-IRES-GFP (RV-CAG-ASCL1-GFP), and Retrovirus CAG::NeuroD1-IRES-GFP (RV-CAG-NeuroD1-GFP).

We initially selected three types of human glioma cell lines—U251 (human astrocytoma, WHO I-III), LN229 (human medulloblastoma, WHO IV), and U87 (human glioblastoma, WHO IV)—for transfection with neural transcription factors. Both ASCL1- and NeuroD1-transfected cells exhibited neuron-like morphological changes (Figure 7A). Specific DCX expression was detected in U251 cells as early as 7 days past infection (DPI) after a single transcription factor transfection, while MAP2, NeuN, and GAD67 were specifically expressed at 30 DPI and 32 DPI (Figures 7B, 7C and S3D), and no longer colocalized with the glial markers GFAP/S100-β (Figure 7D). In high-grade gliomas, there was a relatively low tendency for neuronal conversion. At 7 DPI, LN229 cells specifically expressed DCX (Figure 7B) and minimal MAP2 expression was observed at intermediate stages. The immature neuronal marker TuJ1 was still clearly expressed in the converted cells until 28 DPI, and no positive expression of the mature neuronal marker NeuN was detected (Figure S1). Neuronal conversion of U87 cells was more challenging, as

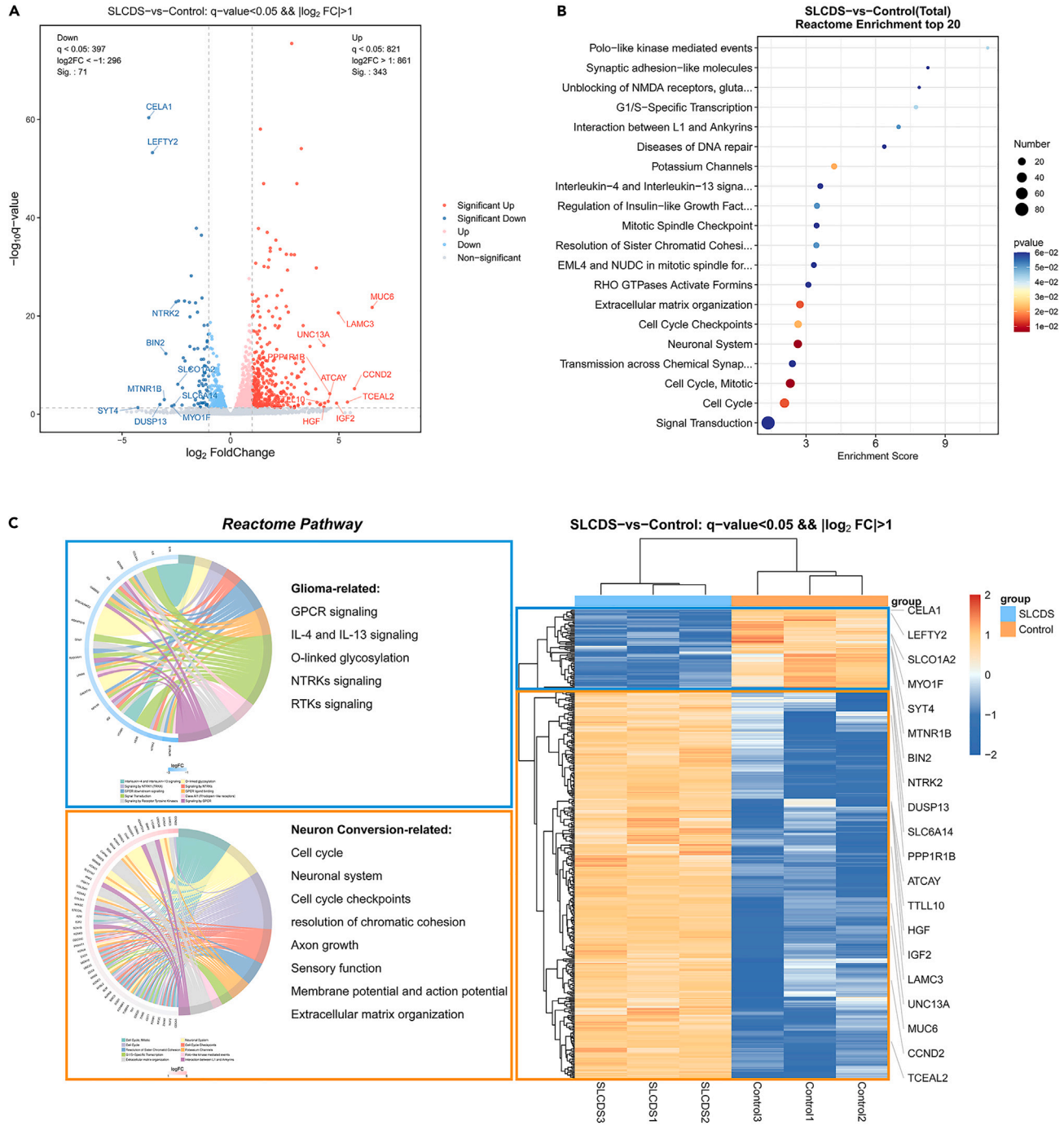

Figure 5. SLCDS upregulated the expression of genes related to neuron conversion, and repressed genes related to glioma

(A) The significant transcriptome change was induced in U251 cells by SLCDS at 14 DPI. The study identified 343 significantly upregulated genes and 71 significantly downregulated genes. Genes were deemed significantly changed when $p < 0.05$ and log2 FC > 1.

(B) Reactome enrichment top 20 of differential expressed genes.

(C) The differential gene expression and related functional changes induced by SLCDS were observed at 14 DPI. The differential expressed genes underwent Reactome enrichment analysis. The left enrichment analysis and the chord diagram respectively listed the downregulated and upregulated differential genes, displaying the 10 classifications with the lowest p value. The graph was divided into left and right sides: the left side displayed the 10 genes with the largest | log2 FC | in each classification, while the right side reflected the composition of classification. The middle lines indicated the correspondence between classifications and genes, and the outer heatmap displayed the log2 FC value of the corresponding gene. $p < 0.05$, log2 FC > 1 indicate statistically significant differences in genes.

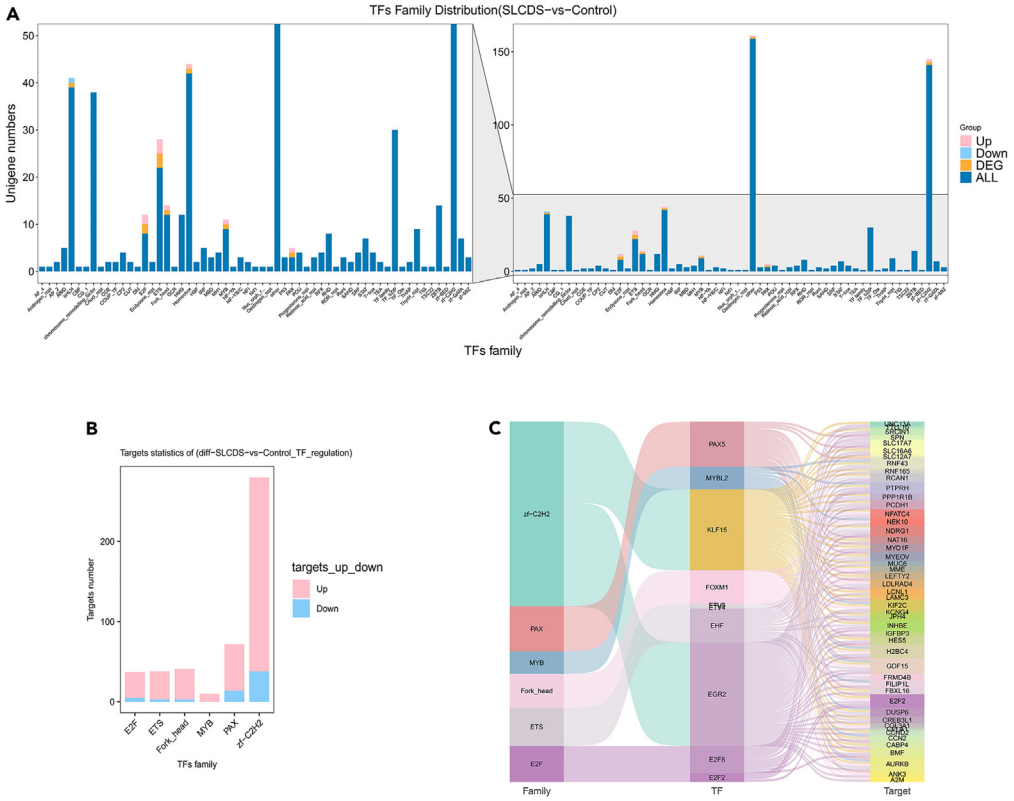

Figure 6. The expression of genes associated with neural transcription factors was significantly upregulated in U251 cells with SLCDS at 14 DPI, leading to the expression of differentially regulated genes downstream of the transcription factors

(A) Diagram of differential transcription factor family distribution. The horizontal axis represents the transcription factor family; the vertical axis represents the number of genes; dark blue represents all genes regulated by a family of transcription factors; orange represents differential transcription factors regulated by a family of transcription factors; pink represents differential transcription factors regulated by a family of transcription factors with a trend of up regulation; light blue represents differential transcription factors regulated by a family of transcription factors with a trend of downregulation.

(B) Distribution display of transcription factor family target genes. Abscissa is the transcription factor family; the ordinate is the number of target genes; pink represents target genes with a trend of upregulation; blue represents target genes with a trend of downregulation; values represent the number of up/downregulated genes.

(C) A Sankey diagram of differential transcription factors—target genes. From left to right: The first column is the transcription factor family; the second column is the differential transcription factors; the third column is the differential target genes. The middle lines indicate the relationships among transcription factor family, transcription factor and target gene. The top 10 transcription factors and the top 50 target genes corresponding to | log2 FC | were selected for mapping.

TuJ1 and DCX expression were not observed until 28 and 35 DPI, respectively, and MAP2 and NeuN expression were not detected throughout the process (Figure S2). We also validated the expression after transfection with neural transcription factors, and the results showed that overexpression of neural transcription factors occurred in U251, LN229, and U87 (Figures S3 A, S3B, and S3C).

Primary cells from a patient diagnosed with postoperative human oligodendroglioma (WHO III) were then selected and subcultured for at least five passages to eliminate any remaining neurons, neural precursor cells, and neuroblasts. After RV transfection, the glioma cells were placed in neuronal differentiation medium (NDM). At 28 DPI, some of the RV-CAG-ASCL1-GFP infected cells exhibited rounded cell bodies that had shrunk and lacked characteristic cellular protrusions. GFP-positive cells showed specific expression of MAP2 and NeuN, with some cells co-labeled with GFP, MAP2, and NeuN. Similarly, some of the RV-CAG-NeuroD1-GFP infected cells displayed rounded and shrunken cell bodies, with more prominent cell protrusions visible. GFP (+) cells also exhibited specific expression of MAP2 and NeuN, with some cells co-labeled with GFP, MAP2, and NeuN. In cells co-infected with RV-CAG-ASCL1-GFP and RV-CAG-NeuroD1-GFP, GFP (+) cells displayed a characteristic neuron-like morphology, mostly co-labeled with GFP, MAP2, and NeuN (Figure 8A). At 64 DPI, the ASCL1, NeuroD1, and ASCL1 + NeuroD1 transfected cells all exhibited obvious neuron-like morphology, with the "multipolar" cells of ASCL1 + NeuroD1 appearing more mature (Figure 8B). We cultured the converted cells *in vitro* for up to 81 days, and we observed various trends. MAP2 expression was decreased in NeuroD1 transfected cells and was only visualized at the soma, but not in the ASCL1 transfected cells, where NeuN was not significantly expressed, and neurites were significantly retracted. MAP2 expression was more pronounced in NeuroD1 + ASCL1 transfected cells, where MAP2 staining was clearly observed in neurites, even at subtle terminal protrusions, and MAP2 (+) cells specifically expressed NeuN at the same time (Figure 8C). Cells transfected with two neural transcription factors, NeuroD1 and ASCL1, were able to grow steadily

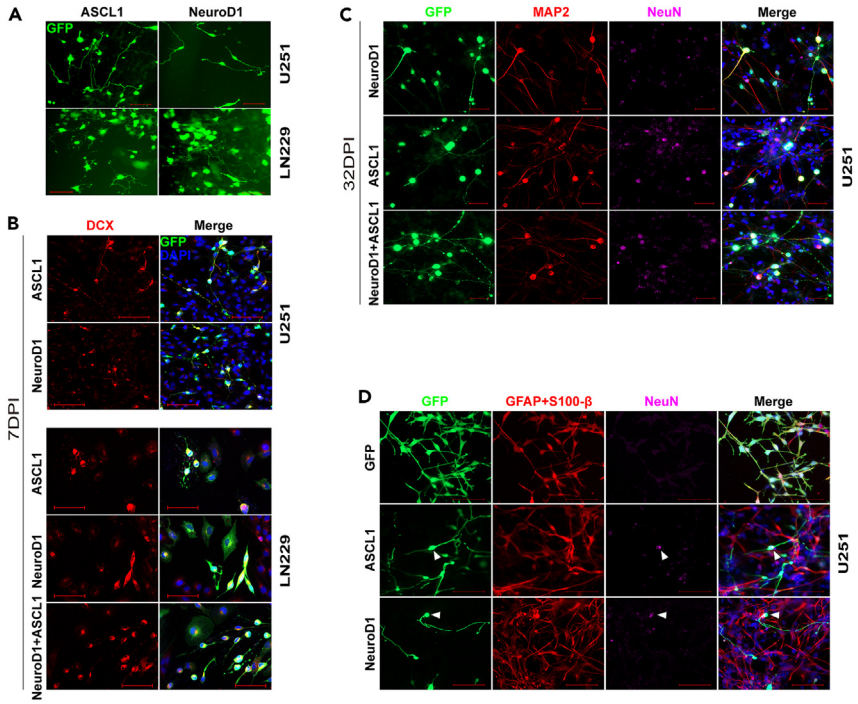

Figure 7. The overexpression of neural transcription factors induced the conversion of human glioma cell lines into neurons

(A) Retroviral expression of ASCL1 or NeuroD1 induced neuron-like morphological changes in the human glioma cell lines U251 and LN229. Scale bar: 100 μm.

(B) Both U251 and LN229 cells were induced into early-stage neurons by NeuroD1 and ASCL1 at 7 DPI. Scale bar: 100 μm.

(C) Transfection of ASCL1 and NeuroD1 with retroviruses induced the conversion of U251 cells into mature neuron-like cells at 32 DPI. Scale bar: 100 μm.

(D) Retroviral expression of transcription factors inhibited glioma-associated proteins and upregulated neuronal markers expression in U251 cells at 30 DPI. Scale bar: 100 μm.

and mature for an extended period of time. At 4 weeks past infection (WPI), whole-cell patch-clamp recordings showed that ASCL1-transfected cells exhibited continuous action potentials and sodium-potassium currents, along with a certain level of spontaneous synaptic activity (Figures 8D, 8E, and 8F).

DISCUSSION

In the current study, we identified a combination of small molecules with the potential to induce glioma neuronal conversion. Through *in vitro* induction, SLCDS were able to convert human glioma cells into mature inhibitory neuronal subtypes, which exhibited significant inhibitory effects on proteins closely associated with glioma proliferation, angiogenesis, invasion, and metastasis. During conversion, the upregulation of neural transcription factors such as NeuroD1 and Sox2 was detected. SLCDS was also found to upregulate the expression of TF genes related to neurogenesis and tumor suppression, thereby activating neurogenesis related biological functions while suppressing glioma related biological functions. We have finally demonstrated in multiple gliomas that overexpression of neural transcription factors can induce the conversion of glioma cells into neurons.

Previous studies have shown that small molecules have a significant impact on converting glial cells into functional mature neurons, and several groups have utilized small molecules to induce this conversion.[38–40] To achieve this, we experimented with CORE, which has demonstrated efficacy in converting glial cells into neurons. We discovered that gliomas are more resistant to conversion compared to normal glial cells, and the resulting neurons are challenging to further mature, consistent with findings from other research groups. In the studies currently published, researchers have been able to use small molecules to induce the conversion of glioma cell lines into early neuron-like cells in humans or mice.[11,12] During the small molecule screening process using CORE, we discovered that CORE + SKL2001 had significant advantages over CORE alone in inducing glioma conversion at an early stage. Further studies have revealed that SLCDS not only induced the conversion of human glioma cells into early neuron-like cells with high efficiency at the initial stage, but also that a certain number of converted cells gradually developed mature neuron-like characteristics and even expressed markers of inhibitory neuronal subtypes. We investigated the expression of specific neuronal markers (DCX, TuJ1, MAP2, NeuN, and GAD67) at various stages. Increasing the concentration of SLCDS enhanced the conversion process, and SLCDS outperformed CORE at all stages in terms of both conversion efficiency and maturation of converted cells. It was also the first time that glioma cells were converted into mature neuron-like cells through small molecule induction and differentiated into various subtypes of neurons. SKL2001 is a novel agonist of the Wnt/β-Catenin signaling pathway.[18] The Wnt pathway plays a crucial role in embryonic development, especially in the central nervous system. This pathway is closely related to the distribution of axial

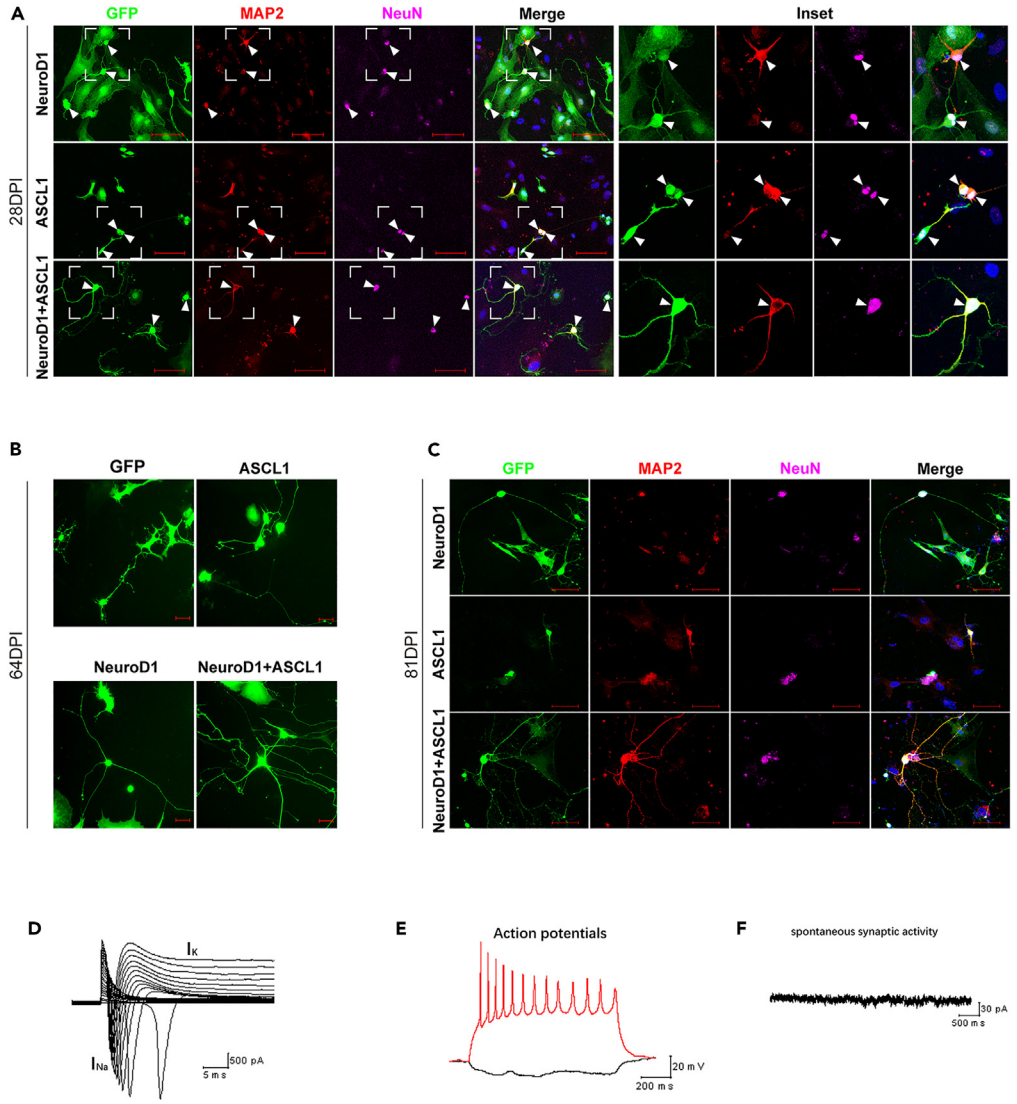

Figure 8. Overexpression of neural transcription factors induced the conversion of human primary glioma cells to neurons

(A) Human primary glioma cells were converted into mature neuron-like cells after retroviral expression of ASCL1, NeuroD1, or both at 28 DPI. Scale bar: 100 μm.

(B) Human primary glioma cells underwent changes in cell morphology and density after retroviral expression of neural transcription factors. Scale bar: 50 μm.

(C) The mature neuron-like cells, which were converted by neurol TF-transfected human primary glioma cells, remained stable at 81 DPI. Scale bar: 100 μm.

(D) Neural electrophysiology was performed on ASCL1-infected GFP (+) human primary glioma cells at 4 WPI, controls were human primary glioma cells not transfected with neurol TFs. Typical sodium and potassium currents were detected at the membrane of ASCL1-converted cells.

(E) Continuous release of action potentials was detected in ASCL1-converted cells.

(F) Some level of spontaneous synaptic activity was recorded in ASCL1-converted cells.

structures in the central nervous system and the differentiation of anterior and posterior brain structures.[41–43] During the investigation of small molecule induced neuronal conversion of glial cells, it was observed that the Wnt pathway was significantly upregulated without the direct action of Wnt pathway activators.[13] In addition, a series of neural transcription factors (e.g., Hes5, Neurog1, Neurog2, NeuroD1, nhlh1, NeuroD2, NeuroD6, bhlhe22, ASCL1, etc.) showed upregulated RNA expressions, while conversely glia related transcription factors were downregulated.[13] This discovery initially explained the mechanism of small molecules inducing the conversion of glial cells into neurons and established a connection between small molecules and transcription factors. We further found that SLCDS strongly enhanced the protein expression of neural transcription factors NeuroD1 and Sox2. Additionally, SLCDS upregulated the RNA expression of a series of neural-related transcription factors, promoted neurogenesis, and suppressed tumor related genes. Evidence of transcriptional upregulation of certain neural transcription factors, such as Brn2, ASCL1, and Neurog2, has also been reported in other studies.[12] The small molecules currently used in neuronal conversion are all primarily cell signaling pathway regulators, which play a crucial role in determining the expression

of transcription factors as important upstream links. This may also be the reason why small molecules can influence the expression of transcription factors.

It can be observed at almost all stages of conversion that the total number of cells induced by SLCDS was significantly reduced. Additionally, the Ki67 (+)/DAPI (+) ratio, which represents cell proliferation,[44] was significantly lower, and these effects were also enhanced with the increase in SLCDS concentration. This suggests that SLCDS inhibits the proliferative capacity of glioma cells. The inhibition of glioma by SLCDS was also demonstrated through the downregulation of certain tumor markers, such as EGFR, PDGFR, and vimentin, which are closely related to the processes of angiogenesis, invasion, and metastasis in glioma.[45–47] The inhibitory effects were further enhanced by the increased concentration of SLCDS. This discovery is somewhat more thrilling than the capability of SLCDS to induce neuronal conversion. In previous studies, no significant inhibition of gliomas by small molecules was observed.[11,12] Although the suppression of glioma has been observed in neural transcription factor transfection, it is limited to inhibiting the proliferative capacity of transfected cells.[3–7] We also discovered that the transcription of gene pathways primarily involved in glioma signaling, proliferation, invasion, migration, and angiogenesis was significantly downregulated at the early stage of conversion. This aspect has been largely unexplored in previous studies. The tumor is a condition in which a specific cell loses its normal regulation of cell proliferation at the genetic level due to various carcinogenic factors, leading to abnormal proliferation.[48] It is well known that gliomas have a significantly higher proliferative capacity than normal cells. It is still difficult to curb the overall rate of tumor development solely by converting glioma cells into neurons; however, inhibiting glioma growth while inducing glioma neuronal conversion might be a more ideal strategy for glioma treatment.

We successfully overexpressed neural transcription factors by retroviral transfection of ASCL1 and NeuroD1 encoding into multiple grade glioma cells. We discovered that both high- and low-grade gliomas (WHO I-IV) can exhibit varying degrees of neuronal conversion. As early as 2012, Jiao Jianwei's group demonstrated that human glioma cells underwent gradual neuron-like changes and expressed neural markers when cultured *in vitro* and transfected with lentivirus carrying ASCL1, Brn2, and Neurog2 encoding.[3] Since then, several teams have made similar attempts.[4–7] The results are exciting, but there are still unanswered questions. Most studies have shown positive results in low-grade gliomas, such as U251, but not in high-grade gliomas, particularly glioblastoma or medulloblastoma of WHO IV. No convincing evidence has emerged thus far. In addition, most of the viral vectors that achieve satisfactory effects are lentiviruses or retroviruses. However, their potential for use in the clinical treatment of glioma is limited due to the transfection mechanisms that integrate coding on the genome of target cells and their associated toxic side effects.[49] These results also illustrate that the upregulation of neural transcription factors expression could drive glioma cells to neuronal cells. Furthermore, they support the idea that the neural conversion effect of SLCDS might be related to its upregulation of a series of neural transcription factors in glioma cells.

In conclusion, our study confirms that SLCDS can activate the overexpression of neural transcription factors in human glioma cells and induce the conversion of human glioma cells into mature neuron-like cells. Additionally, SLCDS have significant inhibitory effects on proteins and genes associated with the proliferation, angiogenesis, and invasion functions of gliomas. Our study is the first to report the conversion of gliomas into mature neuron-like cells induced by small molecules, offering a new potential treatment for glioma patients.

Limitations of the study

Several limitations in our study should be considered. The most major limitation is that research is currently limited to the validation of *in vitro* experiments, whereas achieving conversion *in vivo* is our ongoing research endeavor. Small molecule translational studies have so far remained mainly focused on *in vitro* experiments, with very few involving *in vivo* experiments, probably mainly because of the problems of encapsulation and release of small molecules in *in vivo* models in order to maintain similar drug conditions as in *in vitro* experiments. This requires multidisciplinary co-operation with materials science, pharmacology and other disciplines. Secondly, in our experiments only astrocytomas were verified to be induced by SLCDS to convert into neuron-like cells, whereas there did not seem to be a similar effect on other types of gliomas. This may be related to differences in the TFs required for the conversion of different cells and may require the involvement of other small molecules, but our results still add to the evidence for small molecule conversion in gliomas. Thirdly, although we observed an increase in the expression of nTFs during the conversion process, the precise mechanism underlying conversion remains elusive and represents a key focus of our forthcoming research.

RESOURCE AVAILABILITY

Lead contact

Further information and requests for resources and reagents should be directed to and will be fulfilled by the lead contact, Xiangyu Wang (wang_xy123@126.com).

Materials availability

This study did not generate new unique reagents.

Data and code availability

- RNA-seq data have been deposited at GEO and are publicly available as of the date of publication. Accession numbers are listed in the key resources table. Microscopy data reported in this paper will be shared by the lead contact upon request.
- All original R code generated for Differentially Expressed Genes Analysis is available in this paper's supplemental information.
- Any additional information required to reanalyze the data reported in this paper is available from the lead contact upon request.

ACKNOWLEDGMENTS

This study was supported by the National Natural Science Foundation of China, no. 81472052; the Natural Science Foundation of Guangdong Province of China, no. 2020A1515010854; the Fundamental Research Funds for the Central Universities, 21623307; the China Postdoctoral Science Foundation 2023M741384, the Funding by Science and Technology Projects in Guangzhou, 2024A04J3936.

We would like to express our gratitude to Professor Gong Chen for his invaluable support and guidance, and to Dr Jiancheng Liao for his assistance with the experimental process and materials.

AUTHOR CONTRIBUTIONS

Material preparation and data collection were performed by Y.Y. and W.C. Data analysis was performed by P.X. and C.M. The literature search was performed by Q.W. The first draft of the manuscript was written by Y.Y. X.W. and Z.L. critically revised the manuscript. All authors commented on previous versions of the manuscript. All authors read and approved the final manuscript. X.W., Q.W., and J.L. contributed to the study's conception and design.

DECLARATION OF INTERESTS

The authors declare no competing interests.

STAR★METHODS

Detailed methods are provided in the online version of this paper and include the following:

- KEY RESOURCES TABLE
- EXPERIMENTAL MODEL AND STUDY PARTICIPANT DETAILS
- METHOD DETAILS
  - Conversion of glioma cells into neurons
  - Immunocytochemistry
  - Patch-clamp recordings in cell cultures
  - RNA sequencing and Differentially Expressed Genes Analysis
- QUANTIFICATION AND STATISTICAL ANALYSIS

SUPPLEMENTAL INFORMATION

Supplemental information can be found online at https://doi.org/10.1016/j.isci.2024.111091.

Received: March 12, 2024
Revised: June 25, 2024
Accepted: September 29, 2024
Published: October 2, 2024

REFERENCES

1. Louis, D.N., Ohgaki, H., Wiestler, O.D., Cavenee, W.K., Burger, P.C., Jouvet, A., Scheithauer, B.W., and Kleihues, P. (2007). The 2007 WHO Classification of Tumours of the Central Nervous System. Acta Neuropathol. *114*, 97–109.
2. Carli, E.D. (2009). IDH1 and IDH2 mutations in gliomas. N. Engl. J. Med. *360*, 765–773.
3. Zhao, J., Hua, H., Zhou, K., Ren, Y., Shi, Z., Wu, Z., Wang, Y., Lu, Y., and Jiao, J. (2012). Neuronal Transcription Factors Induce Conversion of Human Glioma Cells to Neurons and Inhibit Tumorigenesis. PLoS One *7*, e41506.
4. Su, Z., Zang, T., Liu, M.L., Wang, L.L., Niu, W., and Zhang, C.L. (2014). Reprogramming the fate of human glioma cells to impede brain tumor development. Cell Death Dis. *5*, e1463. https://doi.org/10.1038/cddis.2014.425.
5. Cheng, X., Tan, Z., Huang, X., Yuan, Y., Qin, S., Gu, Y., Wang, D., He, C., and Su, Z. (2019). Inhibition of Glioma Development by ASCL1-Mediated Direct Neuronal Reprogramming. Cells *8*, 571.
6. Cheng, Y., Liao, S., Xu, G., Hu, J., Guo, D., Du, F., Contreras, A., Cai, K.Q., Peri, S., Wang, Y., et al. (2020). NeuroD1 Dictates Tumor Cell Differentiation in Medulloblastoma. Cell Rep. *31*, 107782.
7. Wang, X., Pei, Z., Hossain, A., Bai, Y., and Chen, G. (2020). Transcription factor-based gene therapy to treat glioblastoma through direct neuronal conversion. Cancer Biol Med *18*, 860–874.
8. Hou, P., Li, Y., Zhang, X., Liu, C., Guan, J., Li, H., Zhao, T., Ye, J., Yang, W., Liu, K., et al. (2013). Pluripotent stem cells induced from mouse somatic cells by small-molecule compounds. Science *341*, 651–654. https://doi.org/10.1126/science.1239278.
9. Li, Q., Ma, Z., Qin, S., and Zhao, W.J. (2023). Virtual Screening-Based Drug Development for the Treatment of Nervous System Diseases. Curr. Neuropharmacol. *21*, 2447–2464. https://doi.org/10.2174/1570159x20666220830105350.
10. Cheng, L., Gao, L., Guan, W., Mao, J., Hu, W., Qiu, B., and Zhao, J. (2015). Direct Conversion of Astrocytes into Neuronal Cells by Drug Cocktail. Cell research *25*, 1269–1272. 细胞研究.
11. Jinsoo, O., Kim, Y., Che, L., Kim, J.B., Chang, G.E., Cheong, E., Kang, S.G., and Ha, Y. (2017). Regulation of cAMP and GSK3 signaling pathways contributes to the neuronal conversion of glioma. PLoS One *12*, e0178881.
12. Christopher, L., Meghan, R., and Michelle, W.S. (2018). Direct Reprogramming of Glioblastoma Cells into Neurons Using Small Molecules. ACS Chem. Neurosci. *9*, 3175–3185. https://doi.org/10.1021/acschemneuro.8b00365.
13. Ma, N.X., Yin, J.C., and Chen, G. (2019). Transcriptome Analysis of Small Molecule–Mediated Astrocyte-to-Neuron Reprogramming. Front. Cell Dev. Biol. *7*, 82.
14. Laping, N.J., Grygielko, E., Mathur, A., Butter, S., Bomberger, J., Tweed, C., Martin, W., Fornwald, J., Lehr, R., Harling, J., et al. (2002). Inhibition of transforming growth factor (TGF)-beta1-induced extracellular matrix with a novel inhibitor of the TGF-beta type I receptor kinase activity: SB-431542. Mol. Pharmacol. *62*, 58–64. https://doi.org/10.1124/mol.62.1.58.
15. Sanvitale, C.E., Kerr, G., Chaikuad, A., Ramel, M.C., Mohedas, A.H., Reichert, S., Wang, Y., Triffitt, J.T., Cuny, G.D., Yu, P.B., et al. (2013). A new class of small molecule inhibitor of BMP signaling. PLoS One *8*, e62721. https://doi.org/10.1371/journal.pone.0062721.
16. Naujok, O., Lentes, J., Diekmann, U., Davenport, C., and Lenzen, S. (2014). Cytotoxicity and activation of the Wnt/beta-catenin pathway in mouse embryonic stem cells treated with four GSK3 inhibitors. BMC Res. Notes *7*, 273. https://doi.org/10.1186/1756-0500-7-273.
17. Luo, X., Tan, H., Zhou, Y., Xiao, T., Wang, C., and Li, Y. (2013). Notch1 signaling is involved in regulating Foxp3 expression in T-ALL.

Cancer Cell Int. *13*, 34. https://doi.org/10.1186/1475-2867-13-34.
18. Gwak, J., Hwang, S.G., Park, H.S., Choi, S.R., Park, S.H., Kim, H., Ha, N.C., Bae, S.J., Han, J.K., Kim, D.E., et al. (2012). Small molecule-based disruption of the Axin/β-catenin protein complex regulates mesenchymal stem cell differentiation. Cell Res. *22*, 237–247. https://doi.org/10.1038/cr.2011.127.
19. Moore, D.L., Apara, A., and Goldberg, J.L. (2011). Kruppel-like transcription factors in the nervous system: novel players in neurite outgrowth and axon regeneration. Mol. Cell. Neurosci. *47*, 233–243. https://doi.org/10.1016/j.mcn.2011.05.005.
20. Otteson, D.C., Liu, Y., Lai, H., Wang, C., Gray, S., Jain, M.K., and Zack, D.J. (2004). Kruppel-like factor 15, a zinc-finger transcriptional regulator, represses the rhodopsin and interphotoreceptor retinoid-binding protein promoters. Invest. Ophthalmol. Vis. Sci. *45*, 2522–2530. https://doi.org/10.1167/iovs.04-0072.
21. Ray, R.S., Corcoran, A.E., Brust, R.D., Soriano, L.P., Nattie, E.E., and Dymecki, S.M. (2013). Egr2-neurons control the adult respiratory response to hypercapnia. Brain Res. *1511*, 115–125. https://doi.org/10.1016/j.brainres.2012.12.017.
22. Yiu, E.M., and Baets, J. (2015). Chapter 16 - Congenital and Early Infantile Neuropathies (Neuromuscular Disorders of Infancy, Childhood, and Adolescence).
23. Chu, X.J., Du, K., Meng, L.C., Xie, Z.Y., Zhu, Y., Zhang, W., Wang, Z.X., and Yuan, Y. (2022). EGR2-related mixed demyelinating and axonal Charcot-Marie-Tooth disease: An electrodiagnostic, nerve imaging, and histological study. Clin. Neuropathol. *41*, 245–252. https://doi.org/10.5414/NP301460.
24. Mirsky, R., and Jessen, K.R. (2009). Schwann Cell Development. Encyclopedia of Neuroscience, 463–473.
25. Urbanek, P., Fetka, I., Meisler, M.H., and Busslinger, M. (1997). Cooperation of Pax2 and Pax5 in midbrain and cerebellum development. Proc. Natl. Acad. Sci. USA *94*, 5703–5708. https://doi.org/10.1073/pnas.94.11.5703.
26. Adams, B., Dörfler, P., Aguzzi, A., Kozmik, Z., Urbánek, P., Maurer-Fogy, I., and Busslinger, M. (1992). Pax-5 encodes the transcription factor BSAP and is expressed in B lymphocytes, the developing CNS, and adult testis. Genes Dev. *6*, 1589–1607.
27. Ohtsuka, N., Badurek, S., Busslinger, M., Benes, F.M., Minichiello, L., and Rudolph, U. (2013). GABAergic neurons regulate lateral ventricular development via transcription factor Pax5. Genesis *51*, 234–245. https://doi.org/10.1002/dvg.22370.
28. Liu, Y., and Zhang, Y. (2019). ETV5 is Essential for Neuronal Differentiation of Human Neural Progenitor Cells by Repressing NEUROG2 Expression. Stem Cell Rev. Rep. *15*, 703–716. https://doi.org/10.1007/s12015-019-09904-4.
29. Rios, A.S., Paula De Vincenti, A., Casadei, M., Aquino, J.B., Brumovsky, P.R., Paratcha, G., and Ledda, F. (2022). Etv4 regulates nociception by controlling peptidergic sensory neuron development and peripheral tissue innervation. Development *149*, dev200583. https://doi.org/10.1242/dev.200583.
30. Fontanet, P.A., Ríos, A.S., Alsina, F.C., Paratcha, G., and Ledda, F. (2018). Pea3 Transcription Factors, Etv4 and Etv5, Are Required for Proper Hippocampal Dendrite Development and Plasticity. Cerebr. Cortex *28*, 236–249. https://doi.org/10.1093/cercor/bhw372.
31. Liu, D., Liu, Z., Liu, H., Li, H., Pan, X., and Li, Z. (2016). Brain-derived neurotrophic factor promotes vesicular glutamate transporter 3 expression and neurite outgrowth of dorsal root ganglion neurons through the activation of the transcription factors Etv4 and Etv5. Brain Res. Bull. *121*, 215–226.
32. Fontanet, P., Irala, D., Alsina, F.C., Paratcha, G., and Ledda, F. (2013). Pea3 transcription factor family members Etv4 and Etv5 mediate retrograde signaling and axonal growth of DRG sensory neurons in response to NGF. J. Neurosci. *33*, 15940–15951. https://doi.org/10.1523/JNEUROSCI.0928-13.2013.
33. Sakamoto, K., Endo, K., Sakamoto, K., Kayamori, K., Ehata, S., Ichikawa, J., Ando, T., Nakamura, R., Kimura, Y., Yoshizawa, K., et al. (2021). EHF suppresses cancer progression by inhibiting ETS1-mediated ZEB expression. Oncogenesis *10*, 26. https://doi.org/10.1038/s41389-021-00313-2.
34. Reehorst, C.M., Nightingale, R., Luk, I.Y., Jenkins, L., and Mariadason, J.M. (2021). EHF is essential for epidermal and colonic epithelial homeostasis and suppresses Apc -initiated colonic tumorigenesis. Development *148*, dev199542.
35. Park, C., Lee, I., and Kang, W.K. (2006). Influence of small interfering RNA corresponding to ets homologous factor on senescence-associated modulation of prostate carcinogenesis. Mol. Cancer Therapeut. *5*, 3191–3196. https://doi.org/10.1158/1535-7163.MCT-06-0570.
36. Taniue, K., Oda, T., Hayashi, T., Okuno, M., and Akiyama, T. (2011). A member of the ETS family, EHF, and the ATPase RUVBL1 inhibit p53-mediated apoptosis. EMBO Rep. *12*, 682–689. https://doi.org/10.1038/embor.2011.81.
37. Chow, A., Amemiya, Y., Sugar, L., Nam, R., and Seth, A. (2012). Whole-transcriptome analysis reveals established and novel associations with TMPRSS2:ERG fusion in prostate cancer. Anticancer Res. *32*, 3629–3641.
38. Hu, W., Qiu, B., Guan, W., Wang, Q., Wang, M., Li, W., Gao, L., Shen, L., Huang, Y., Xie, G., et al. (2015). Direct Conversion of Normal and Alzheimer's Disease Human Fibroblasts into Neuronal Cells by Small Molecules. Cell Stem Cell *17*, 204–212.
39. Zhang, L., Yin, J.C., Yeh, H., Ma, N.X., Lee, G., Chen, X.A., Wang, Y., Lin, L., Chen, L., and Jin, P. (2015). Small Molecules Efficiently Reprogram Human Astroglial Cells into Functional Neurons. Cell Stem Cell *17*, 735–747.
40. Gao, L., Guan, W., Wang, M., Wang, H., Yu, J., Liu, Q., Qiu, B., Yu, Y., Ping, Y., Bian, X., et al. (2017). Direct Generation of Human Neuronal Cells from Adult Astrocytes by Small Molecules. Stem Cell Rep. *8*, 538–547.
41. Mcmahon, A.P., and Bradley, A. (1990). The Wnt-1 (int-1) proto-oncogene is required for development of a large region of the mouse brain. Cell *62*, 1073–1085.
42. Thomas, K.R., and Capecchi, M.R. (1990). Targeted disruption of the murine int-1 proto-oncogene resulting in severe abnormalities in midbrain and cerebellar development. Nature *346*, 847–850.
43. Zhou, C.J., Pinson, K.I., and Pleasure, S.J. (2004). Severe Defects in Dorsal Thalamic Development in Low-Density Lipoprotein Receptor-Related Protein-6 Mutants. J. Neurosci. *24*, 7632–7639.
44. Nielsen, L.A.G., Bangsø, J.A., Lindahl, K.H., Dahlrot, R.H., Hjelmborg, J.v.B., Hansen, S., and Kristensen, B.W. (2018). Evaluation of the proliferation marker Ki-67 in gliomas: Interobserver variability and digital quantification. Diagn. Pathol. *13*, 38. https://doi.org/10.1186/s13000-018-0711-2.
45. An, Z., Aksoy, O., Zheng, T., Fan, Q.-W., and Weiss, W.A. (2018). Epidermal growth factor receptor and EGFRvIII in glioblastoma: signaling pathways and targeted therapies. Oncogene *37*, 1561–1575. https://doi.org/10.1038/s41388-017-0045-7.
46. Cao, Y. (2013). Multifarious functions of PDGFs and PDGFRs in tumor growth and metastasis. Trends Mol. Med. *19*, 460–473. https://doi.org/10.1016/j.molmed.2013.05.002.
47. Satelli, A., and Li, S. (2011). Vimentin in cancer and its potential as a molecular target for cancer therapy. Cell. Mol. Life Sci. *68*, 3033–3046. https://doi.org/10.1007/s00018-011-0735-1.
48. J.C.E., U. (2000). General and Systematic Pathology, 3th ed. (Churchilllivingstone).
49. Somia, N. (2004). Gene delivery to cells in culture using retroviruses. Methods Mol. Biol. *246*, 491–498.
50. Bolger, A.M., Lohse, M., and Usadel, B. (2014). Trimmomatic: a flexible trimmer for Illumina sequence data. Bioinformatics *30*, 2114–2120. https://doi.org/10.1093/bioinformatics/btu170.
51. Kim, D., Langmead, B., and Salzberg, S.L. (2015). HISAT: a fast spliced aligner with low memory requirements. Nat. Methods *12*, 357–360. https://doi.org/10.1038/nmeth.3317.
52. Roberts, A., Trapnell, C., Donaghey, J., Rinn, J.L., and Pachter, L. (2011). Improving RNA-Seq expression estimates by correcting for fragment bias. Genome Biol. *12*, R22. https://doi.org/10.1186/gb-2011-12-3-r22.
53. Trapnell, C., Williams, B.A., Pertea, G., Mortazavi, A., Kwan, G., Baren, M., Salzberg, S.L., Wold, B.J., and Pachter, L. (2010). Transcript assembly and quantification by RNA-Seq reveals unannotated transcripts and isoform switching during cell differentiation. Nat. Biotechnol. *28*, 511–515.
54. Anders, S., Pyl, P.T., and Huber, W. (2015). HTSeq–a Python framework to work with high-throughput sequencing data. Bioinformatics *31*, 166–169. https://doi.org/10.1093/bioinformatics/btu638.
55. Anders, S., and Huber, W. (2012). Differential expression of RNA-Seq data at the gene level – the DESeq package. Heidelberg, Germany: European Molecular Biology Laboratory (EMBL) *10*, f1000research.
56. David, C., Fabregat, M.A., Robin, H., Marija, M., Joel, W., Wu, G., Michael, C., Phani, G., Marc, G., and Kamdar, M.R. (2014). The Reactome pathway knowledgebase. Nucleic Acids Res. *42*, D472–D477.

STAR★METHODS

KEY RESOURCES TABLE

REAGENT or RESOURCE	SOURCE	IDENTIFIER
Antibodies		
Doublecortin (DCX)	Abcam	Cat# ab18723; RRID: AB_732011
Doublecortin (DCX)	Millipore	Cat# AB2253; RRID: AB_1586992
Doublecortin (DCX)	Abnova	Cat# H00001641-M01; RRID: AB_463920
EGF Receptor	CST	Cat# 4267; RRID: AB_2246311
GABA AFFINITY ISOLATED	Sigma-Aldrich	Cat# A2052; RRID: AB_477652
GABA AFFINITY ISOLATED	Sigma-Aldrich	Cat# A0310; RRID: AB_476667
GAD67	Millipore	Cat# MAB5406; RRID: AB_2278725
GAD67	SYSY	Cat# 198 013; RRID: AB_2107718
GFAP	Sigma-Aldrich	Cat# G3893; RRID: AB_477010
GFAP	Sigma-Aldrich	Cat# G9269; RRID: AB_477035
GFAP	Invitrogen	Cat# 13-0300; RRID: AB_2532994
GFP	Invitrogen	Cat# A-11122; RRID: AB_221569
GFP	Invitrogen	Cat# A-11120; RRID: AB_221568
GFP	Abcam	Cat# ab13970; RRID: AB_300798
Ki67	Abcam	Cat# ab15580; RRID: AB_443209
MAP2	Millipore	Cat# AB5622; RRID: AB_91939
MAP2	Abcam	Cat# ab5392; RRID: AB_2138153
Mash1(Ascl1)	BD Bioscience	Cat# 556604; RRID: AB_396479
NeuN	Millipore	Cat# ABN90; RRID: AB_11205592
NeuN	Novus	Cat# NBP1-92693; RRID: AB_11036146
NeuN	Abcam	Cat# ab177487; RRID: AB_2532109
NeuroD1	Abcam	Cat# ab60704; RRID: AB_943491
PDGFRα	Santa Cruz	Cat# sc-338; RRID: AB_631064
Sox2	Abcam	Cat# ab79351; RRID: AB_10710406
Sox2	Millipore	Cat# AB5603; RRID: AB_2286686
S-100β	Abcam	Cat# ab52642; RRID: AB_882426
TuJ-1/tubbulin β-3	Convance/biolegened	Cat# PRB-435P-100; RRID: AB_291637
TuJ-1/tubbulin β-3	Sigma-Aldrich	Cat# T8660; RRID: AB_477590
VGLUT1(BNPI)	SYSY	Cat# 135 302; RRID: AB_887877
VGLUT2	Frontier institute	Cat# VGluT2-GP, RRID: AB_2571621
Vimentin	Millipore	Cat# MAB3400; RRID: AB_94843
Bacterial and virus strains		
Retrovirus CAG-GFP (RV-CAG-GFP)	this paper	N/A
Retrovirus CAG:ASCL1-IRES-GFP (RV-CAG-ASCL1-GFP)	this paper	N/A
Retrovirus CAG::NeuroD1-IRES-GFP (RV-CAG-NeuroD1-GFP)	this paper	N/A
Chemicals, peptides, and recombinant proteins		
SB431542	Sigma-Aldrich	CAS No.: 909089-13-0
LDN193189	Sigma-Aldrich	CAS No.: 1062368-24-4
CHIR99021	Sigma-Aldrich	CAS No.: 252917-06-9

(*Continued on next page*)

Continued

REAGENT or RESOURCE	SOURCE	IDENTIFIER
DAPT	Sigma-Aldrich	CAS No.: 208255-80-5
SKL2001	Sigma-Aldrich	CAS No.: 909089-13-0
Forskolin	Sigma-Aldrich	CAS No.: 66575-29-9
GDNF	GIBCO	Product # 450-10-10UG
Dorsomorphin	Sigma-Aldrich	CAS No.: 866405-64-3
BDNF	GIBCO	Product # 450-02-1MG
NT3	GIBCO	Product # 450-03-10UG
Y-27632	Tocris	Cat#1254
IGF-1	Cell Signaling	Cat#3093
Critical commercial assays		
mirVana miRNA Isolation Kit	Ambion	AM1561
TruSeq Stranded mRNA LT Sample Prep Kit	Illumina	https://www.illumina.com.cn/products/by-type/sequencing-kits/library-prep-kits/truseq-stranded-mrna.html
Deposited data		
RNA-seq data	GEO	https://www.ncbi.nlm.nih.gov/geo/submitter/ Accession numbers : GSE262741
Experimental models: Cell lines		
U-251MG	ATCC	RRID:CVCL_0021
U-87MG	ATCC	RRID:CVCL_0022
LN-229	ATCC	RRID:CVCL_0393
Primary glioma cells	a gift from Dr. Jiancheng Liao	N/A
Software and algorithms		
ZEN Viewer software	Carl Zeiss	https://www.zeiss.com/microscopy/en/products/software/zeiss-zen.html
pClamp 9 software	Molecular Devices	https://support.moleculardevices.com/s/article/Axon-pCLAMP-9-Electrophysiology-Data-Acquisition-Analysis-Software-Download-Page
MiniAnalysis software	Synaptosoft	http://bluecell.co.kr/theme/theme05/product/product_02_05.php
R Statistical Software	v4.3.2, 2023-10-31	https://www.r-project.org
Other		
Epifluorescent microscope	Carl Zeiss	Axio Imager Z2
Confocal microscope	Carl Zeiss	LSM 880
Patch-clamp amplifier	Molecular Devices	https://support.moleculardevices.com/s/article/Axon-MultiClamp-700A-Commander-Download-page Multiclamp 700A
NanoDrop 2000 spectrophotometer	Thermo Scientific	https://assets.thermofisher.com/TFS-Assets/CAD/manuals/NanoDrop-2000-User-Manual-EN.pdf
Agilent 2100 Bioanalyzer	Agilent Technologies	https://www.agilent.com.cn/zh-cn/product/automated-electrophoresis/bioanalyzer-systems/bioanalyzer-instrument/2100-bioanalyzer-instrument-228250

(*Continued on next page*)

Continued

REAGENT or RESOURCE	SOURCE	IDENTIFIER
Illumina platform	Illumina	https://www.illumina.com.cn/content/dam/illumina-marketing/apac/china/documents/hiseq-x-%e7%b3%bb%e5%88%97%e6%b5%8b%e5%ba%8f%e7%b3%bb%e7%bb%9f.pdf HiSeq X Ten

EXPERIMENTAL MODEL AND STUDY PARTICIPANT DETAILS

Human glioma cell lines (U251, U87 and LN229) were purchased from ATCC. The U251 cell line was derived from astrocytoma (male, 75years), refer to U-251MG (RRID:CVCL_0021), while U87 and LN229 were both derived from glioblastoma (male, Age unspecified; female, 60years), database refer to U-87MG ATCC (RRID:CVCL_0022) and LN-229 (RRID:CVCL_0393). Cells were cultured in a culture medium containing DMEM/F12 (GIBCO), 10% FBS (GIBCO) and 1% penicillin/streptomycin (GIBCO).

Primary glioma cells derived from a patient (female, 46years) with a postoperative pathological diagnosis of human oligodendroglioma (WHO III) were a gift from Dr. Jiancheng Liao (ethics review by the Medical Ethics Committee of the First Affiliated Hospital of Jinan University, [2018] Ethics Approval No. 024). Cells were cultured in medium containing 50% DMEM/F12 (GIBCO), 40% Neurobasal (GIBCO), 10% FBS (GIBCO),10 μM forskolin (Sigma), 10 ng/mL GDNF (GIBCO) and 1% penicillin/streptomycin (GIBCO).

For subculture, cells were trypsinized with 0.25% trypsin (GIBCO), centrifuged for 5 min at 1000 rpm, resuspended and plated in a corresponding culture medium at a split ratio of approximately 1:3. Cells were maintained at 37°C in humidified air containing 5% CO_2.

METHOD DETAILS

Conversion of glioma cells into neurons

U251 cells were initially exposed to small molecules for either 4 or 7 days, followed by a transition to NDM supplemented with DMEM/F12, 0.25% FBS, 0.8% N2 (GIBCO), 0.4% B27 (GIBCO), 10 μM forskolin, 1 μM dorsomorphin (Sigma), 20 ng/mL BDNF (GIBCO), 10 ng/mL GDNF, 10 ng/mL NT3 (GIBCO), 1 μM Y27632 (Tocris), 5 μg/mL vitamin C (Selleck Chemicals), 1.7 μM insulin (Sigma) and 20 ng/mL IGF-1 (Cell Signaling) for specified durations prior to immunostaining. The small molecule medium was refreshed every 4 days, and the NDM was half changed every 3 days. SLCDS small molecule medium contained Han's F12 (GIBCO), 0.8% B27, 0.4% N2, 5 μM SB431542 (Sigma), 0.25 μM LDN193189 (Sigma), 1.5 μM CHIR99021 (Sigma), 5 μM DAPT (Sigma), 40 μM SKL2001 (Sigma), and 1.7 μM insulin. CORE small molecule medium contained Han's F12, 0.8% B27, 0.4% N2, 5 μM SB431542, 0.25 μM LDN193189, 1.5 μM CHIR99021, 5 μM DAPT, and 1.7 μM insulin. Primary glioma cells, U251, U87 and LN229 cells were infected with retroviruses expressing NeuroD1-GFP, ASCL1-GFP or GFP alone. The next day, the culture medium was completely replaced by NDM, or 0.2% DMSO (Invitrogen) for control.

Immunocytochemistry

Cultured cells were fixed in 4% PFA in PBS for 15 min at room temperature. The cells were first washed three times with PBS and then pretreated with 0.1% Triton X-100 (Sigma) in PBS for 30 min, followed by incubation with 3% normal goat serum (GIBCO), 2% normal donkey serum (Sigma), and 0.1% Triton X-100 in PBS for 1 h. Primary antibodies were incubated with the cultures overnight at 4°C in 3% normal goat serum, 2% normal donkey serum, and 0.1% Triton X-100 in PBS. After washing in PBS, the samples were incubated with appropriate secondary antibodies conjugated to Alexa Fluor 488, Alexa Fluor 546 or Alexa Fluor 647 (1:300, Molecular Probes) for 1 h at room temperature, followed by washing in PBS. Finally, coverslips were mounted on glass slides using an anti-fading mounting solution containing DAPI (Invitrogen). Slides were first examined by Epifluorescent microscope (Carl Zeiss Axio Imager Z2) and further analyzed by a confocal microscope (Carl Zeiss LSM 880). Z-stacks of digital images, which can either release individual confocal images or collapse into a single resulting image, were acquired and analyzed using ZEN Viewer software (Carl Zeiss).

Patch-clamp recordings in cell cultures

For glioma cell-converted neurons, whole-cell recordings were performed using Multiclamp 700A patch-clamp amplifier (Molecular Devices, Palo Alto, CA), and the chamber was constantly perfused with a bath solution containing 128 mM NaCl, 30 mM glucose, 25 mM HEPES, 5 mM KCl, 2 mM $CaCl_2$, and 1 mM $MgCl_2$. The pH of the bath solution was adjusted to 7.3, and the osmolarity was to 315–325 mOsm/l. Patch pipettes were made of borosilicate glass (3–5 MU) and filled with a pipette solution consisting of 135 mM KCl, 5 mM Na-phosphocreatine, 10 mM HEPES, 2 mM EGTA, 4 mM MgATP, and 0.5 mM Na2GTP (pH 7.3). The series resistance was typically 10–30 MU. For voltage-clamp experiments, the membrane potential was typically held at −70 or −80 mV. NMDA currents were recorded in Mg^{2+} free bath solution (128 mM NaCl, 30 mM D-glucose, 25 mM HEPES, 5 mM KCl, and 2 mM $CaCl_2$ [pH 7.3]) plus 10 mM glycine, 0.5 mM TTX, and 20 mM BIC. Data were acquired using pClamp 9 software (Molecular Devices, Palo Alto, CA), sampled at 10 kHz, and filtered at 1 kHz. Na^+ and K^+ currents and action potentials were analyzed using pClamp 9 Clampfit software. Spontaneous synaptic events were analyzed using MiniAnalysis software (Synaptosoft, Decator, GA). All experiments were performed at room temperature.

RNA sequencing and Differentially Expressed Genes Analysis

Total RNA was extracted using the mirVana miRNA Isolation Kit (Ambion) following the manufacturer's instructions. RNA purity and quantification were evaluated using the NanoDrop 2000 spectrophotometer (Thermo Scientific, USA). RNA integrity was assessed with the Agilent 2100 Bioanalyzer (Agilent Technologies, Santa Clara, CA, USA), and only samples with an RNA Integrity Number (RIN) of 7 or higher were included in further analysis. Libraries were prepared using the TruSeq Stranded mRNA LT Sample Prep Kit (Illumina, San Diego, CA, USA) according to the protocol provided. Sequencing of these libraries was carried out on the Illumina platform (Illumina HiSeq X Ten) to produce 150bp paired-end reads. Raw data (raw reads) of fastq format were first processed using Trimmomatic[50] and the low-quality reads were removed to obtain the clean reads. Then clean reads for each sample were retained for subsequent analyses. The clean reads were mapped to the human genome (GRCh38) using HISAT2.[51] FPKM[52] of each gene was calculated using Cufflinks,[53] and the read counts of each gene were obtained by HTSeqcount.[54] Differential expression analysis was performed using the DESeq (2012) R package.[55] p value <0.05 and fold change >2 or fold change <0.5 were set as the threshold for significant differential expression. Hierarchical cluster analysis of differentially expressed genes (DEGs) was performed to demonstrate the expression pattern of genes in different groups and samples. Reactome[56] enrichment analysis of DEGs was performed respectively using R based on the hypergeometric distribution.

QUANTIFICATION AND STATISTICAL ANALYSIS

Cell counting was performed by taking images at several randomly chosen fields per coverslip and analyzed using ImageJ software. Data were represented as mean ± SEM. Student's t test was used for the comparison between two groups of data. One-way ANOVA and post hoc tests were used for statistical analysis of data from multiple groups. Unless otherwise stated, all figures presented in the text were compared with the control group.